ACS APPLIED POLYMER MATERIALS

Organotin in Nonchemically Amplified Polymeric Hybrid Resist Imparts Better Resolution with Sensitivity for Next-Generation Lithography

Jerome Peter, Mohamad G. Moinuddin, Subrata Ghosh, Satinder K. Sharma,* and Kenneth E. Gonsalves*

Cite This: *ACS Appl. Polym. Mater.* 2020, 2, 1790−1799

Read Online

ACCESS | Metrics & More | Article Recommendations | Supporting Information

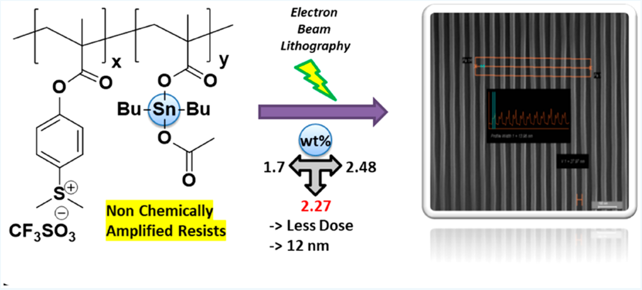

ABSTRACT: Given the need for a next-generation technology node in the area of integrated circuits (ICs), improvement in the properties of resist materials, particularly sensitivity (E_D), resolution, good etch resistance, and low line edge/width roughness (LER/LWR), has been highly desirable but also extremely challenging. Herein, we report a series of organic−inorganic hybrid nonchemically amplified copolymer resists (n-CARs) bearing radiation-sensitive sulfonium functionality as well as tin metal as an organometallic unit in the structural backbone for low E_D and LER/LWR. These resists have been synthesized by the free radical copolymerization of the organic monomer (4-(methacryloyloxy)phenyl)-dimethylsulfoniumtriflate (MAPDST) and acetyldibutylstannyl methacrylate (ADSM) in different feed ratios (97:3, 93:7, 88:12) and characterized using FT-IR, ^1H, ^{19}F NMR, GPC, XPS, and ICP-OES techniques. These MAPDST-*co*-ADSM copolymers exhibited molecular weights (M_w) in the range of 10 077−12 187 g mol^{-1}. Electron beam lithography (EBL) studies revealed that the negative tone n-CARs characteristic with patterning down to sub-15 nm features. The well-developed sub-15 nm nanofeatures showed low LER of ~1.29 ± 0.07 line patterns (number belongs to feed ratio 93:7). The variable e-beam exposure dose study revealed that the E_D of these resists varies with the percentage of incorporated Sn in the polymer matrix. Incorporation of 2.48 wt % Sn (feed ratio 88:12) in the polymer chain led to a significant enhancement in the E_D(175 μC/cm^2). Furthermore, the mechanistic study of pattern development has been performed with electron beam reactivity analyses using the XPS technique. These investigations substantiate the potential candidature of developed resist formulation for next-generation semiconductor technology applications.

KEYWORDS: *hybrid polymer, nonchemically amplified resists, e-beam lithography, high-resolution patterning, <15 nm technology node, metrology*

1. INTRODUCTION

Meeting current market demand for the high performance and functionality of electronic devices is a big challenge for semiconductor industries. Next-generation lithography (NGL)[1] technologies that utilize shorter wavelengths (λ) of irradiation or charged particle beams are being explored extensively to fulfill the resolution requirements of the IRDS-2017.[2,3] As known from the literature, among the various factors that govern the success of NGL techniques, resist materials play an important role. Therefore, considerable efforts have been devoted to photolithography to ease the lithography wavelength from the i-line (λ = 365 nm) to the most progressive extreme ultraviolet (λ = 13.5 nm) radiation for coveted nanopatterning applications.[4] Extreme ultraviolet lithography (EUVL) irradiation complex interactions with novel resist formulations, starting with photoionization that generates primary electrons (~80 eV) and followed by ionization that creates low energy secondary electrons (~10 to 60 eV), are primarily responsible for high-resolution resist patterning to establish NGL.[5] Therefore, the substantiation of high-resolution (HR) patterning competence of new resist formulations toward EBL irradiation is highly desirable to determine the potential candidature of a resist formulation for EUVL applications.

Furthermore, one of the far-reaching factors that makes the NGL process more proficient is the availability of photoresists with sufficiently low line edge/width roughness (LER/LWR)

Received: January 8, 2020
Accepted: April 6, 2020
Published: April 6, 2020

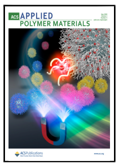

https://dx.doi.org/10.1021/acsapm.0c00005

and exceptionally low exposure dose <10 mJ/cm^2, which has not been achieved simultaneously to date.[5,6] Principally, a resist formulation should exhibit high sensitivity, etch resistance, and high-resolution patterning. A methodical study varying the resist composition, processing conditions, etc., is systematically desired[11−13] to understand the trade-offs among the LER/LWR, sensitivity, and resolution (LSR trade-off).[7−10] As apparently revealed from the exponential growth of the NGL technology, there is an imperative need for advanced organic/inorganic or hybrid resist materials for sub-10 nm technology node patterning.

Recently, Brainard et al. reported molecular hybrid resists based on Pt, Pd, Sn, and Sb metals for HR-EUVL applications.[14,15] Shi et al. reported fullerene-based molecular n-CAR for 10 nm patterning applications.[16] Moreover, Telecky et al. demonstrated hafnium-based metal oxide resist HafSOx for 18 nm line-space (half-pitch) features exposed at 240 μC/cm^2 with LWR of 1.6 nm.[17] Our group recently explored (4-(methacryloyloxy)phenyl)-dimethylsulfoniumtriflate (MAPDST)-based copolymers as radiation/photosensitive resists for sub-15 nm patterning and found them to be suitable at e-beam doses of 1200 μC/cm^2.[10,18−20] In a recent report, Enomoto et al. demonstrated the sensitivity enhancement by introducing the organotin compound in a n-CAR resist prepared typically through a conventional esterification reaction.[21] Notably, electrons of as low as ∼1.2 eV can induce chemical reactions in the Sn-based resist formulation. Therefore, incorporation of Sn as organometallic species may lead to development of highly sensitive e-beam resists.[5] Moreover, there is an increase of more than two times in sensitivity also observed because of the generation of polymer radicals through the Sn−C bond scission.[21] The present work demonstrates the design and development of three new hybrid n-CAR$_s$ resists composed of MAPDST−*co*−ADSM copolymer obtained from polymerization of acetyldibutylstannyl methacrylate (ADSM) and MAPDST at different feed ratio. These negative tone nonchemically amplified resists (n-CAR$_s$) have been used as potential patterning candidates for electron beam lithography (EBL).[10] The synthesized resist showed CD patterning down to 12 nm. Focusing on the heavy metals, particularly tin (Sn), has been of great interest mainly because of its interesting nature such as high optical density (σ_{EUV}) 10−12 and also the hemolysis of C−Sn bond sensitivity is highly significant during the irradiation.[10,19,20] We investigated the effect of various weight percentages of organo-tin (Sn) species in polymer network on HR-EBL patterning. Also, for detailed analysis, a systematic investigation on the effect of patterning and processing parameters on HR pattern generation has been performed.

2. EXPERIMENTAL SECTION

2.1. Chemicals and Reagents. All the standard reagents and chemicals were purchased from commercial sources and used as received. Azobisisobutryronitrile (AIBN) was purchased from Paras Polymers, India and recrystallized twice from methanol before use. MAPDST and ADSM monomers were prepared according to reported procedures.[19,20]

2.2. Procedure for the Synthesis of n-CAR Hybrid Copolymers. MAPDST-co-ADSM Copolymers: The MAPDST:ADSM resists A, B, and C were prepared by reacting the monomers MAPDST and ADSM in three different feed ratios of 97:3, 93:7, and 88:12, respectively.

2.2.1. Resist A. Synthesis procedure for MAPDST-*co*-ADSM: The radiation-sensitive organic monomer MAPDST (0.969 g, 2.607 mmol), tin (Sn)-based monomer ADSM (0.030 g, 0.080 mmol) and AIBN (1 weight%, relative to both the monomers) were taken in a Schlenk flask under a N_2 atmosphere under darkness. To this was added 15 mL of tetrahydrofuran (THF −acetonitrile (ACN) dry solvent mixture (2:1, v/v) under nitrogen atmosphere. Thereafter, the reaction mixture was transferred into a clean oven-dried polymerization flask with a side arm neck via filtering through 0.45 μm Teflon filter. To remove oxygen from the reaction mixture, we conducted several rounds of freeze−thaw cycles (6−7 cycles) with N_2 purging. After that, the reaction mixture was allowed to stir for 2 days at 60 °C. After the completion of the reaction, the mixture was poured slowly into diethyl ether (50 mL) and the separated solid was washed several times with diethyl ether. The resulting crude product was dissolved in methanol and then reprecipitated using diethyl ether. Finally, the separated white product was filtered off and dried in a temperature controlled hot air oven at 50 °C for 1 day. Yield: 490 mg (49%); FT-IR: ν_{max}/cm^{-1} 3022−2859 (CH), 1748 (C═O), 1586−1493 (C═C), 1248 (CF$_3$), 1095−1026 (C−O), 515 (Sn−C). ^{1}H NMR (500 MHz, DMSO-d_6) δ_H 8.02 (br peak, ArH), 7.41 (br peak, ArH), 3.19−3.21(br peak, aliphatic proton), 1.27−1.75 (br peak, aliphatic proton). ^{19}F NMR (376 MHz; DMSO-d_6) δ_F−77.6 (3F, s, CF$_3$).% of Sn = 1.70 (determined from ICP-OES). Calculated ratio of MAPDST (x) and ADSM (y) monomers in polymer network (x:y) = 95:5 (calculation details are provided in Figure S19).

2.2.2. Resist B. The procedure was similar to that followed for resist A, except that the ratio of MAPDST and ADSM used was different. For resist B, 0.929 g of MAPDST (2.499 mmol), 0.071 g of ADSM (0.188 mmol), and AIBN (1 wt %, relative to both monomers) were used. Yield: 520 mg (52%). ^{1}H NMR (500 MHz, DMSO-d_6) δ_H 8.02 (br peak, ArH), 7.41 (br peak, ArH), 3.19−3.21(br peak, aliphatic proton), 1.20−1.50 (br peak, aliphatic proton). ^{19}F NMR (376 MHz; DMSO-d_6) δ_F−77.6 (3F, s, CF$_3$).% of Sn = 2.27 (determined from ICP-OES). Calculated ratio of MAPDST (x) and ADSM (y) monomers in polymer network (x:y) = 93:7 (calculation details are provided in Figure S19).

2.2.3. Resist C. The same procedure as that of resist A was followed using 0.880 g of MAPDST (2.365 mmol), 0.122 g if ADSM (0.322 mmol), and 1 wt % AIBN (relative to both monomers). Yield: 534 mg (53%); ^{1}H NMR (500 MHz, DMSO-d_6) δ_H 8.01 (br peak, ArH), 7.41 (br peak, ArH), 3.19−3.21(br peak, aliphatic proton), 1.10−1.60 (br peak, aliphatic proton. ^{19}F NMR (376 MHz; DMSO-d_6) δ_F−77.6 (3F, s, CF$_3$).% of Sn = 2.48 (determined from ICP-OES). Calculated ratio of MAPDST (x) and ADSM (y) monomers in polymer network (x:y) = 92:8 (calculation details are provided in Figure S19).

2.3. Imaging Experiment. *2.3.1. Resist Processing.* To form a uniform thin film for EBL, we prepared the resist solutions by dissolving 3 wt % of the respective polymers in acetonitrile, and the resulting solutions were centrifuged for complete homogeneity. Foreign particles from resist solutions were filtered through a 0.2 μm Teflon filter two times. The resist solutions were then spin-coated onto 2 in. p-type silicon (100) wafers to get uniform thin films. Films of thickness ∼25 nm (shown in Figure S18a) were achieved by spin coating the resist solution at ∼4500 rpm for 60 s. A pre-exposure bake (PAB) of the resist-coated wafers was performed at 70 °C for 90 s on a hot plate to remove the solvent from the coated resist films. The coated films were exposed using e-beam energy of 20 keV under Raith e-Line PLUS tool. A low aperture of the 10 μm diameter was used for a highly collimated beam with a beam-current of 29.8 pA for high-resolution (HR) patterning onto resist thin films. A variable exposure dose patterning procedure was also adopted for analyzing the cross-linking. LER and inspection of energy fluence effect in MAPDST-*co*-ADSM resist formulations with variation in dose. After exposure, the resist films were optimized to postexposure bake (PEB) at different temperatures of 30, 70, 110, and 150 °C for 60 s to minimize the LER/LWR and patter surface roughness.[22] Finally, the negative tone nanofeatures were achieved after the development of resist films using aqueous TMAH developer of different concentrations (varied from 0.0026 to 0.26 N).[23]

2.3.2. Imaging and Metrology. The developed photoresist patterns were analyzed by in-built FESEM. The remaining thickness

Scheme 1. Synthesis of n-CAR (MAPDST-*co*-ADSM) Formulations

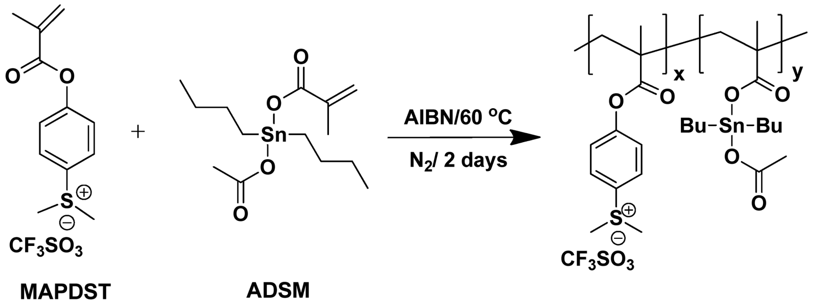

Table 1. Chemical Composition of MAPDST-co-ADSM with Different Feed Ratio

resist	feed ratio (*X*:*Y*)	calculated polymer composition[a,b] (*X*:*Y*)	Sn[b] (%)	average molecular weight[a] (Mw)	poly-dispersity indices[a] (PDI)	decomposition temperature[c] (Td)
A	97:3	95:5	1.70	10,077	1.564	>200
B	93:7	93:7	2.27	11,727	1.503	>200
C	88:12	92:8	2.48	12,187	1.569	>200

[a] Calculated from gel permeation chromatography (GPC). [b] Calculated from inductively coupled plasma optical emission spectrometry (ICP-OES). [c] Calculated from thermo gravimetric analysis (TGA).

of the photoresist was analyzed using atomic force microscopy (AFM) and sensitivity-contrast relation was plotted. The high-resolution EBL pattern micrographs were subjected to industrial standard SUMMIT analytical tool for line-edge roughness (LER)/line-width roughness (LWR) analyses.[24]

2.4. Thin-Film Irradiation. To analyze compositional changes after e-beam interaction, we prepared thin films of MAPDST-*co*-ADSM copolymer (~25 nm thickness) and exposed them to EBL in high current mode with a large write field (1000 × 1000 μm^2) in a 4 × 4 mm^2 area above the critical dose E_D for resist B (2.27% Sn). The exposed/unexposed wafers were postbaked and loaded into X-ray photoelectron spectroscopy. Both the unexposed and exposed samples were characterized with all survey spectra and core spectra of C 1s, F 1s, O 1s, S 2p, and Sn 3d using photon energy fixed at 1200 eV.

2.5. Instrumentation Details. Fourier transform infrared (FT-IR) spectra were recorded by using the PerkinElmer spectrum-2 spectrophotometer. $^1H/^{19}F$ NMR analysis was done using a Jeol JNM ECX 500 MHz nuclear magnetic resonance (NMR) spectrometer in DMSO-d_6/$CDCl_3$ solvents. Molecular weights (M_w) and poly dispersity indexes (PDI) of the hybrid polymers were determined using gel permeation chromatography (GPC) from the Agilent-1260 infinity series. PL gel mixed B with pore size 10 μm was used as a column compartment for the molecular weight determinations. We used 0.1% LiBr in dimethylformamide (DMF) as a mobile phase at the flow rate of 1 mL/min with the column temperature 70 °C. Thermogravimetry (TGA) and differential scanning calorimetry (DSC) analyses were performed by Netzsch model STA 449 F1 JUPITER Series instrument. The heating rate was employed at 10 °C/min in a N_2 atmosphere over a temperature range from 25 to 800 °C. Thickness measurements were performed by using the NanoMap-550 stylus profilometer. Raith e-Line Plus was used as an e-beam patterning tool for nanolithography investigations with a dose range from 100 to 1000 $\mu C/cm^2$. X-ray photoelectron spectroscopy (Thermo-Fisher) was used to analyze the compositional information on the synthesized photoresist before and after exposure conditions. Low-energy Ar^+ cluster (200 eV) plasma was bombarded to remove the native carbon and oxygen without further chemical changes.

3. RESULTS AND DISCUSSIONS

3.1. Synthesis and Characterization. Monomers of MAPDST and ADSM were synthesized following the procedures reported elsewhere and characterized by using ^1H NMR analyses (Figures S1 and S2).[19] The MAPDST organic unit having R_3S^+ group at the para position of a phenyl ring has been proven to be a key component in the development of a series of new hybrid polymers based n-CARs formulations.[18] Thus, herein, a series of MAPDST-*co*-ADSM, copolymers based on different feed ratios of MAPDST and ADSM monomers to enhance the sensitivity of the resists toward e-beam irradiation, have been designed and developed. Accordingly, the MAPDST-*co*-ADSM copolymer were synthesized by the reaction between radiation-sensitive cationic organic moiety MAPDST with organometallic ADSM in acetonitrile/tetrahydrofuran (1:2) solvent mixture using AIBN as a free radical initiator under a nitrogen atmosphere at 60 °C for 2 days. The synthesis route for MAPDST-*co*-ADSM copolymer formulation is given in Scheme 1. The synthesized copolymer resists were characterized by using FT-IR, NMR, gel permeation chromatography (GPC), thermogravimetric analyses (TGA), X-ray photoelectron spectroscopy (XPS), and ICP techniques (see Figures S1−S18). The weight-average molecular weight (M_w) and poly dispersity indices (PDI) of the MAPDST-*co*-ADSM copolymers were calculated from the GPC analysis and found to be 10 077 g/mol^{-1} and 1.56, 11 727 g/mol^{-1} and 1.50, and 12 187 g/mol^{-1} and 1.56 for resists A, B and C, respectively (Figures S14−S17). XPS analyses revealed the presence of tin in polymer samples (Figures S9−S11). The chemical composition of resist A (97:3), B (93:7), and C (88:12) have been tabulated in Table 1. The TGA analyses revealed that the copolymers were stable up to 190 °C and start decomposing after 220 °C, indicating adequate thermal stability of MAPDST-*co*-ADSM resists generally desired for NGL applications (Figure S13). An enhancement in the thermal stability of the copolymers has been observed with the incorporation of organotin complex unit in the polymer backbone as compared to that of the pure organic homopolymer reported earlier.[17] In the FT-IR spectrum of the copolymer, the stretching frequencies at 1748 and 1248 cm^{-1} belong to carbonyl and $-CF_3$ groups, respectively. The band at 515 cm^{-1} indicates the presence of Sn−C bond in the copolymer and further confirms the presence of Sn in the resist formulation.

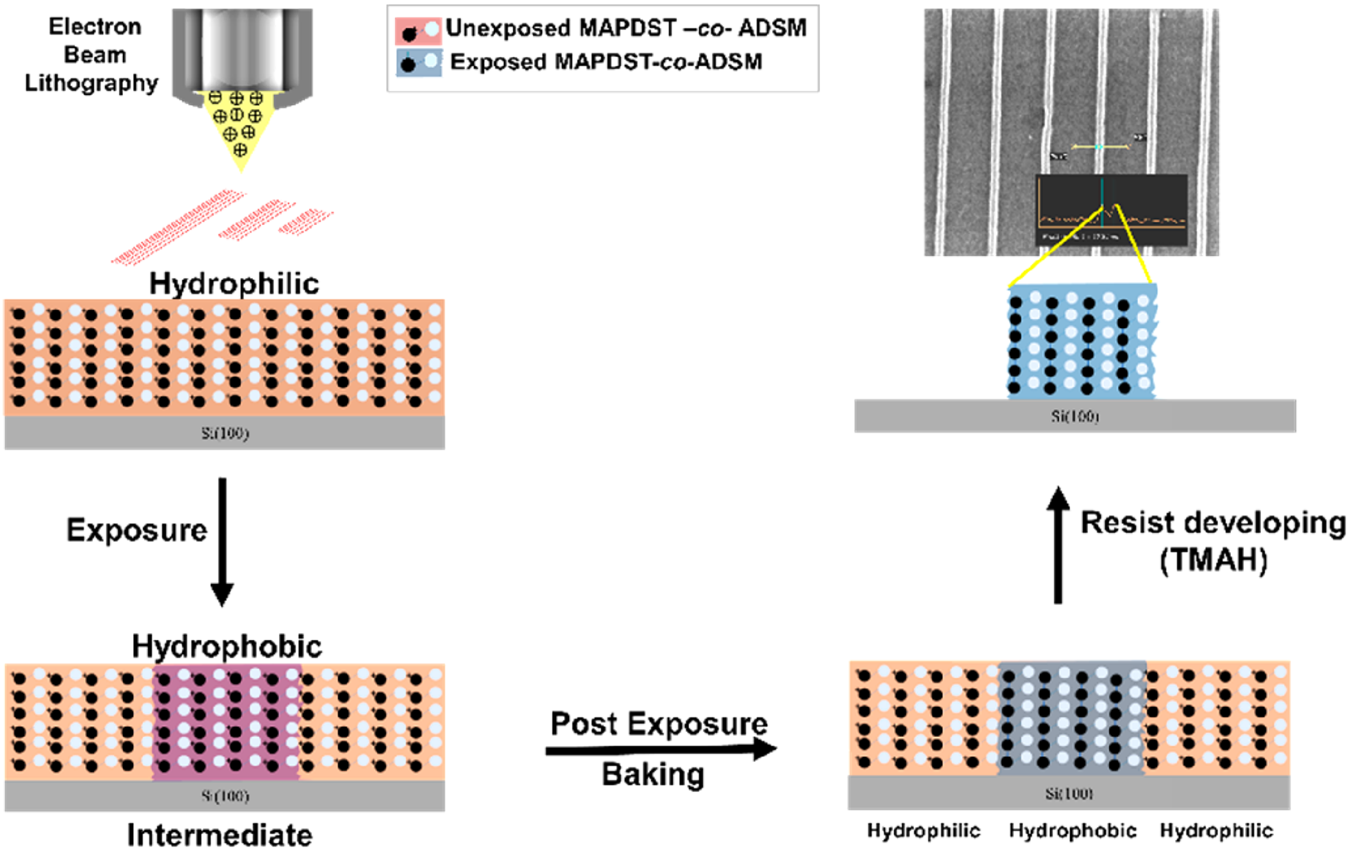

Figure 1. Schematic for e-beam exposure and pattern formation on MAPDST-*co*-ADSM resist formulations.

In ^{1}H NMR spectra of copolymers, the resonance peaks of the olefinic protons of the monomers MAPDST and ADSM appearing at δ 5.97, 6.32 ppm and at δ 5.57, 6.20 ppm, respectively, disappeared.[19] It indicates the transformation of monomers into hybrid copolymers. The resonance signals due to the aromatic protons of MAPDST monomers appearing between 7.58 and 8.15 ppm got up-fielded to 7.41 and 8.04 ppm in the polymer as a broad singlet. The integration values of the signals between δ 1.27 and 1.41 ppm belonging to the polymer backbone protons increase gradually with increasing ADSM feed ratio.[20] These results thus confirm the expected chemical structure of MAPDST-*co*-ADSM copolymers obtained from the free radical polymerization process.

3.2. High-Resolution Pattern Generation from E-Beam Lithography (EBL).

To analyze the critical dose/sensitivity (E_D) and critical dimension (CD) of the MAPDST-*co*-ADSM resist formulations, we explore here the charge-based HR-EBL technique.[25−27] A systematic representation of e-beam exposure and polarity change in the MAPDST-*co*-ADSM resists are explained in Figure 1. To realize low proximity effect inside MAPDST-*co*-ADSM, e-beam was accelerated to 20 keV. The exposure dose was varied from 100 to 1000 μC/cm^2 to analyze the effect of Sn content incorporation in MAPDST-*co*-ADSM resists for well-developed HR-patterning.

Figure 2a shows the variation in resist sensitivity with the addition of ADSM in the photoresist chain. The plotted sensitivity (E_D) variations and model fitting indicates that the E_D is partially inversely proportional to the incorporation of Sn as irradiation sensitizer. This reveals that the lateral energy transport due to metal moiety affects the physiochemical variation in the MAPDST chain and hence reduces the E_D.

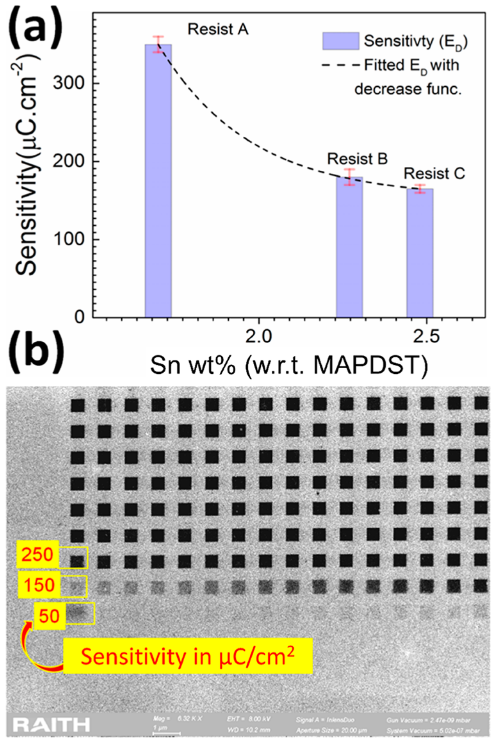

Figure 2. a) Sensitivity curve for MAPDST-*co*-ADSM and (b) NRT with E_D of MAPDST-*co*-ADSM resist B = 200 μC/cm^2.

The variable exposure dose patterning approach adapted for resists formulation sensitivity analysis is shown in Figure 2b,

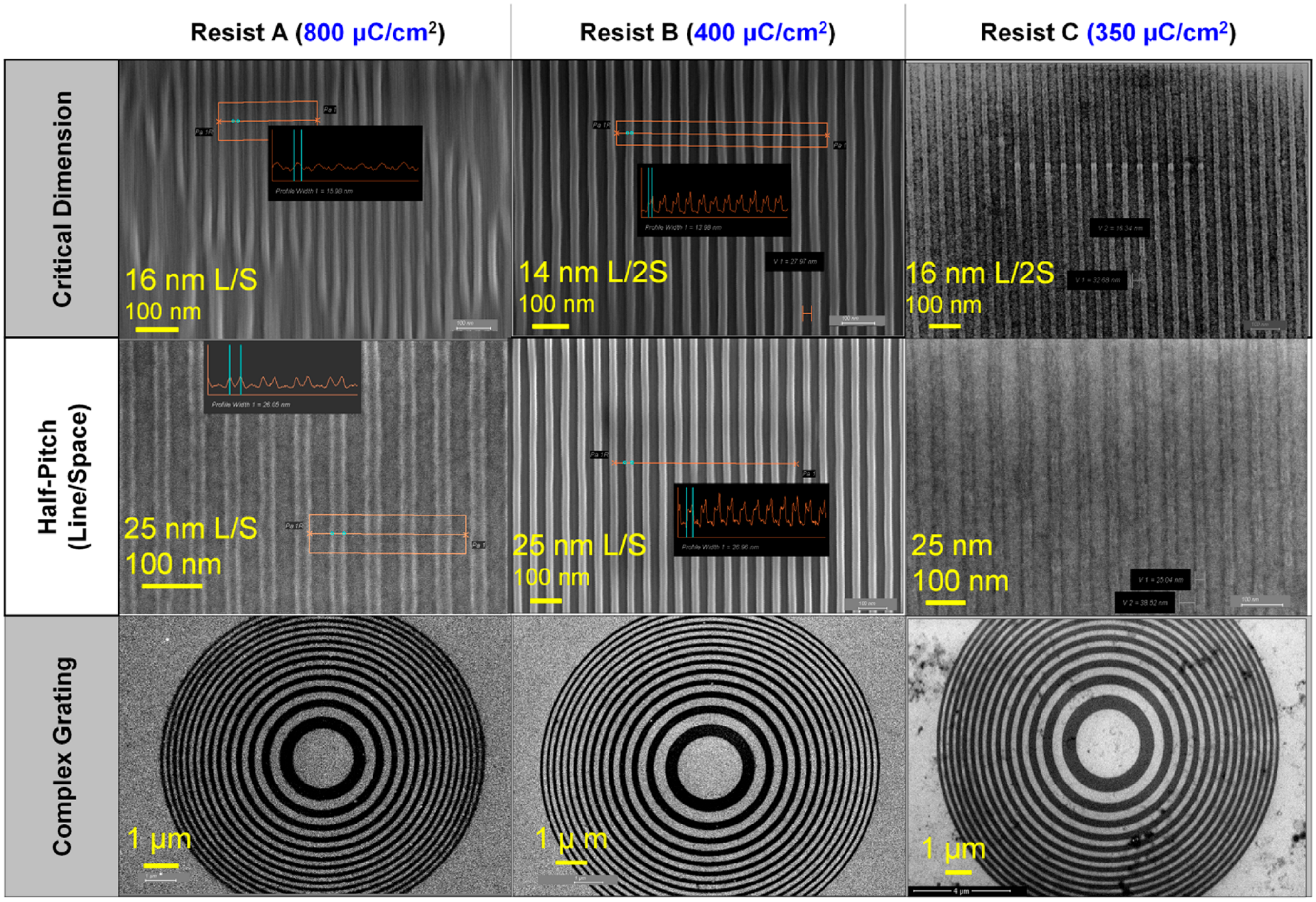

Figure 3. Optimized patterns between resists A, B, and C with different Sn wt %. The modulated E_D of 800, 400, and 350 μC/cm^2 for respective resist compositions; critical dimension (CD) shows the lowest feature and spacing, half-pitch suggest the L/S patterns of 25 nm, and complex patterns show grating with different widtsh.

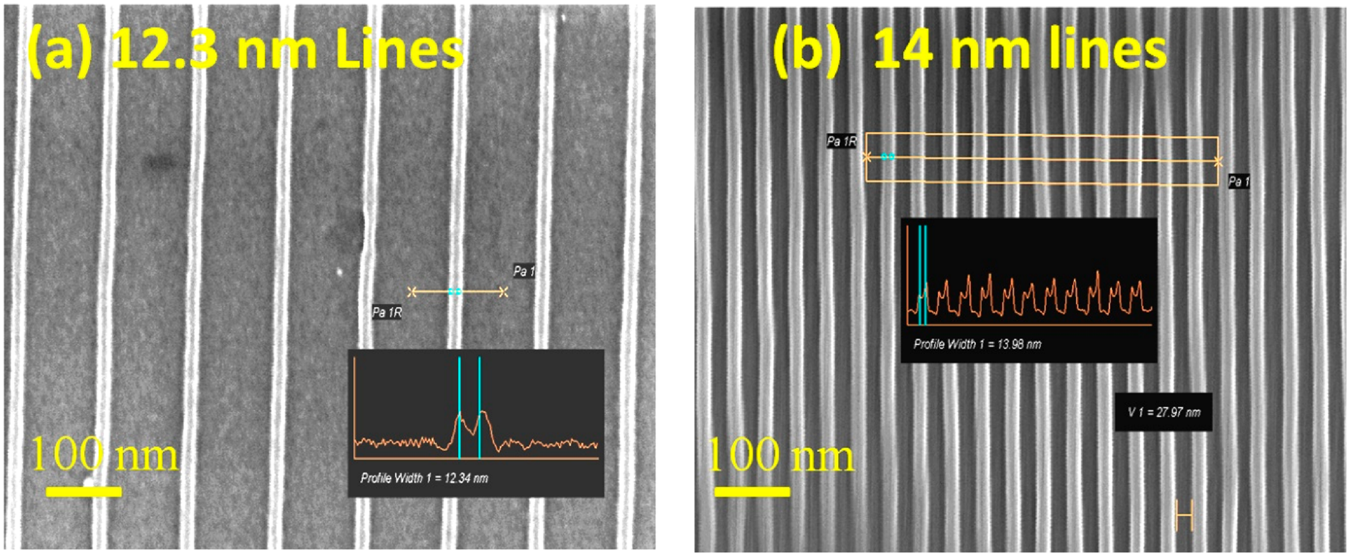

Figure 4. Nanopatterns of resist B with exposed energy of 400 μC/cm^2; (a) 12.3 nm and (b) 14.0 nm with a scale bar of 100 nm.

where the resist was exposed to different energy with a constant difference.

Figure 2a indicates an increase in sensitivity with the increase in tin content in resist sample, as there is a decrease in the E_D from 350 to 175 μC/cm^2 (for 500 nm L/S pads). This distinctly shows that the resist fragmentation kinetics are enhanced by increasing Sn for the same exposure irradiation. It may also be attributed to more irradiation fluence−resist interaction and contribute to the cleavage of Sn−C bond more efficiently through homolysis.[28] The comparative studies

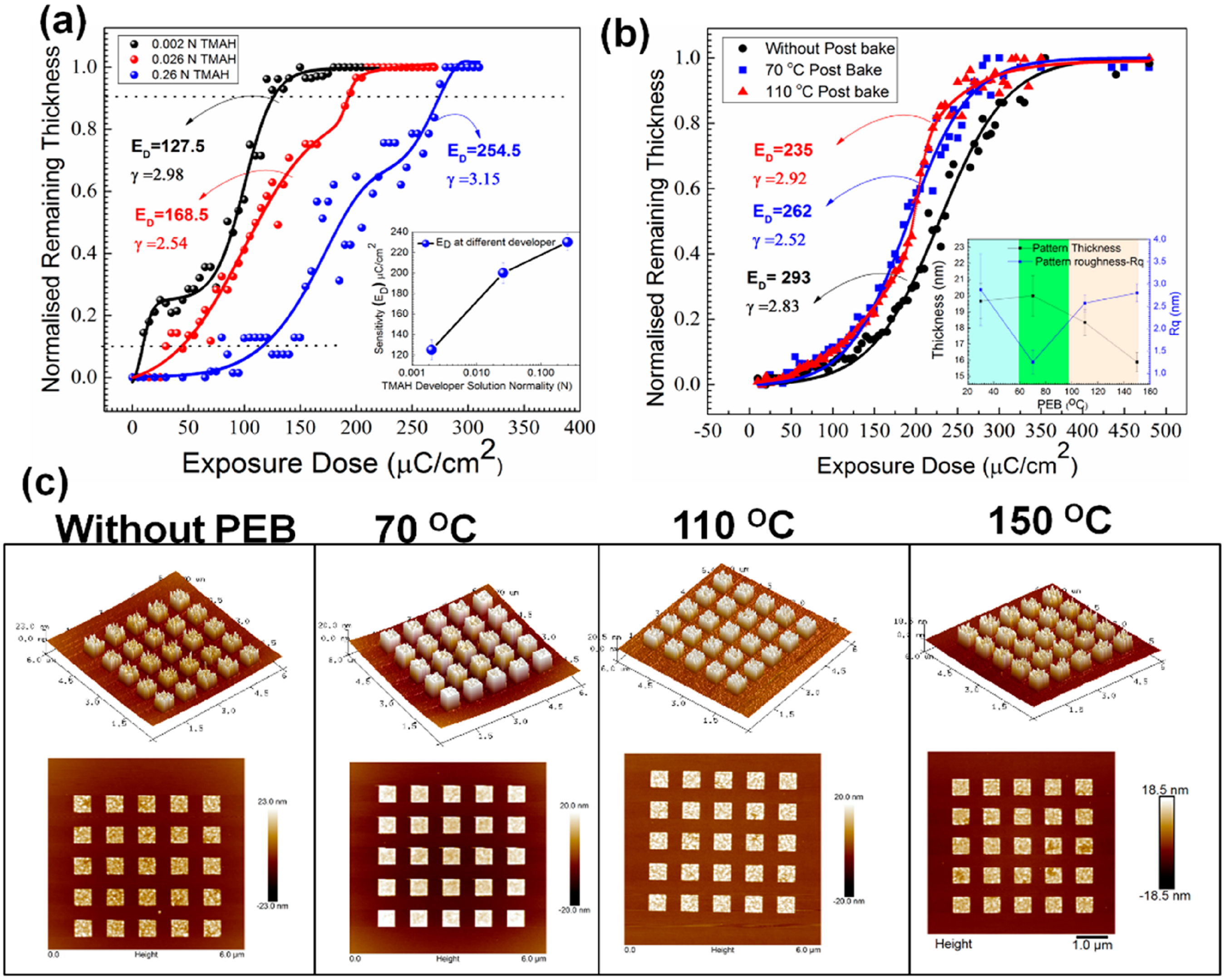

Figure 5. Effect of development parameter on the exposer dose. (a) Sensitivity and contrast curve of MAPDST-*co*-ADSM for different developer concentration; inset shows E_D vs developer; (b) effect of PEB on sensitivity; inset shows the variation of pattern thickness and roughness with PEB, (c) atomic force micrograph of resist patterns at post baked treatment at different temperature (without PEB, 70, 110, and 150 °C).

between the resist A, B, and C formulations in various metrics are illustrated in Figure 3. To establish the sensitivity differences of these resists, it was investigated that resist B at a dose of 400 μC/cm^2 shows sharper images with a good fence profile, which is better than resist formulations A and C. In addition, 25 nm half-pitch patterns of resist B were much better than those of resists A and C. Other than the line features, complex circular patterns could be developed, along with patterns well in line using these resists formulations. It proves that the tin content plays an important role in determining sensitivity, LER/LWR, and high-resolution resist pattern development. At the same time, a delicate balance of tin content is paramount in controlling good solubility of the resist (Figure 3).

Furthermore, the systematic dose analyses for <15 nm features patterning revealed that the lowest critical dimension achieved was ~12.3 nm at a dose of 400 μC/cm^2 (for resist B). Various line patterns (~12, 14, 15 nm, etc.) with different line/space (L/S-L/10S) characteristics exhibited by the hybrid resists. These patterns were characterized using FESEM and micrographs are shown in Figures 3 and 4. The high-resolution EBL patterns of resist B are shown in Figure 4.

The LER and LWR parameters of ~15 nm patterns were calculated using industry standard Summit software (Figure S18). The obtained LER and LWR values were found to be ~1.03 ± 0.07 nm and ~1.18−1.30 nm, which are very much within the acceptable range.[29,30]

3.3. Hybrid n-CARs Dissolution Analysis: Effect of PEB and Developer. The newly synthesized resists were required to be standardized with dissolution rate, which generally depends on the development process and pH of the developer. In the case of negative tone n-CAR formulations, the solubility of the exposed region is in direct relation to the structural changes upon irradiation exposure as compared to the unexposed region. Here, the exposed pattern stability against three different sets of aqueous developer solutions of tetramethylammonium hydroxide (TMAH) having concentrations 0.0026 N (11.78 pH), 0.026 N (12.8 pH) and 0.26 N (13.78 pH) were investigated. Resist C was adapted for these analyses with the expectation that the minimal effect of polarity change will reflect most because of the higher sensitivity than other resist formulations. The relation between the normalized remaining thickness (NRT) and exposer doses at different developer pH is shown in Figure 5a.[31−34] Figure 5a clearly

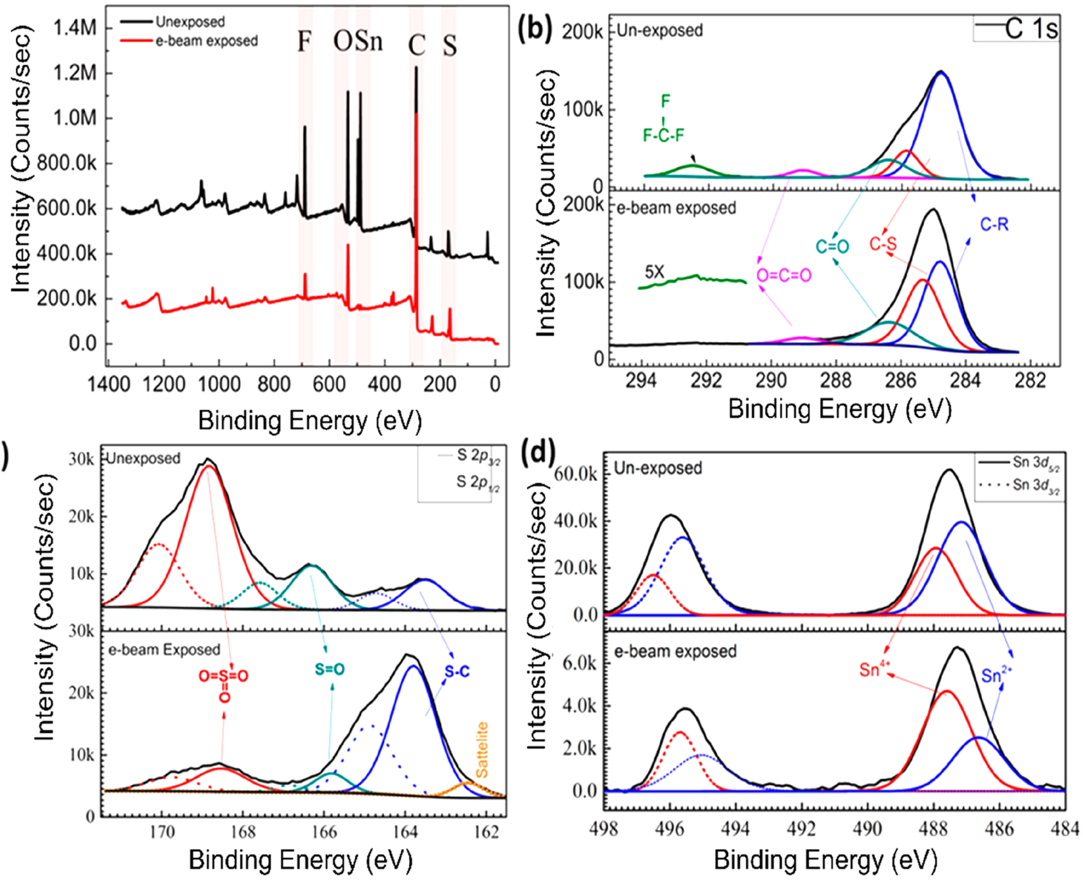

Figure 6. XPS analysis of the e-beam irradiation impact; unexposed and exposed core spectra of (a) survey indicating materials inside MAPDST-*co*-ADSM, (b) C 1s, (c) S 2p, and (d) Sn 3d.

shows that with changing the developer pH, the requirement of E_D also varies gradually. However, more systematic investigations are required to understand the contrast curves. In fact, on increasing the exposure dose to the maximum, initially, the weaker bonds are activated and reacted (π bond to σ bond) but later the strong Sn−C, C−H, and other sigma bonds are affected and the chemical property is completely changing from the hydrophilic to hydrophobic nature (as mentioned in Figure 1), so usually at lower doses, there is more probability of overdevelopment at high pH (0.26N). Therefore, initially, TMAH developer with low pH (0.0026N: closer to DI- pH ∼7) resulted in sufficiently stable patterns at a lower dose. At this developer pH, the unexposed resist area dissolved without affecting the irradiated resist and also considerably enhanced the sensitivity to 127.5 μC/cm^2 (Figure 5a inset) (Figure S20−21). Furthermore, at high pH (∼13.7) developer with 0.26 N, TMAH created much basic media to the resist formulations development, which results in an increased E_D to provide a stable resist pattern. Similar trends were also reported in HSQ resist development when the pH of the developer (TMAH) was varied with the incorporation of salt (NaCl and LiCl).[35−37]

Moreover, to understand the role of the PEB process, we also investigated and plotted the effect of PEB over sensitivity. Figure 5b shows the sensitivity of resist C with different PEB temperatures. There is a small reduction in sensitivity (E_D) with variation PEB temperatures. To establish this, we subjected the samples to PEB at 70 °C, there is a decrease in E_D to ∼262 from 293 μC/cm^2 of without-PEB treated samples. Further, an increase in PEB temperature results in a reduction in E_D but pattern deformation and pattern surface roughness variation are also found to be noticeable. In the case of n-CAR, the irradiation result of the resist bond rearrangement and the generation of stress inside the exposed patterns may lead to pattern collapse.[38] The variation in surface roughness and thickness loss are a major concern for sub-15 nm HR patterning. Figure 5b (inset) shows the variation in surface from the well-developed HR pattering viewpoint, the postbake treatment results the releasing of resist film stress of irradiated patterns and also promote the adhesion between exposed patterns and corresponding substarte. Figure 5b inset shows an improvement on surface roughness when postbaked treatment was followed at 70 °C as compared to without post bake samples. As clearly perceived that the further, increase in temperature up to 150 °C resulted an increase in roughness which may be due to adverse effect of over post back treatement, reduction in adhesion and material loss from resist thin films (25 nm) at the elevated temperatures. To confirm further metrology investigations were performed with AFM of patterned resists as shown in Figure 5c. These outcomes support that ∼70 °C is an optimal temperature for PEB processing of developed resist.

3.4. Electron Beam Reactivity Studies Using E-Beam Flood Exposure. To elucidate the effect of e-beam irradiation, we conducted the mechanistic study on resist formulation before and after EBL irradiation. To understand the binding energy behind the rearrangement of bonds, structural changes, and modulation concerning the atomic

Table 2. Summary and Comparison HR e-Beam Resist

resist		sensitivity (μC/cm^2)	contrast	resolution (nm)	tone	CAR	post baking	industrially optimized	LER/LWR (nm)	ref
HSQ		300– 5000	2.2	02–10	neg.	no	yes	no	3	[42]
CSAR 62		65	14	~6	pos	meth	yes	yes	4.5	[43,44]
PMMA		1.2 nC/cm	4.50	4–8	pos	meth	no	yes	<5	[45]
ma-N 2401		60–160	1.7–2.8	~50		no	yes	no		[46]
mr-EBL6000		2–20	0.7	~80		yes	yes	yes		[46]
SU-8		1–20	0.7–1.7	~30	neg	yes	yes	yes	04–10	[47]
P(HEMA)		0.5–1	1.2	100–200		no	no	no		[48]
ZEP		180	4.18	12	pos	yes		yes		[49]
MAPDST-co-ADSM	97:3	350	1.55	16	neg	no	yes	no	1–3	this work
	93:7	200	2.54	12	neg	no	yes	no	<2	
	88:12	175	2.32	12	neg	no	yes	no	<2	

[a] Abbreviation: neg, negative; pos, positive; meth, methacrylate.

percentage incorporation of Sn entities, we utilized an XPS technique for analysis, and the results are shown in Figure 6. Elemental composition in MAPDST-*co*-ADSM is listed in Figure 6a for unexposed and EBL exposed, followed subsequently for same samples with post-baked treatment at 70 °C. The photoelectron intensities of exposed resist were found to be altered in resist elements such as F, Sn, and O as shown in survey scan Figure 6a. Furthermore, after irradiation under EBL exposure, resists underwent chemical decomposition as shown in Figure 6a, b. A similar fugitive nature of -CF_3 moiety is also observed under in situ photodynamics of MAPDST-homopolymer,[39] whereas a gradual change in the intensities was observed at 168.5 eV ($-SO_3$ group) and ~164 eV ($-SC$ group) after post EBL exposure. Constant intensities above 30k in Figure 6c advocate the minimal degassing of volatile S compound formation in the course of post EBL exposure processing.

The higher irradiation absorption property of the tin-incorporated chemical environment compared to the triflate moiety, which leads to the homolytic dissociation of the Sn−C and Sn−O bonds will be a very important sink for the dissipation of the absorbed high EUV energy. HR-XPS spectra were also recorded for the Sn $3d_{5/2}$ and $3d_{3/2}$ signals and the results are summarized in Figure 6d. After irradiation and oxidation of the films, two new signals at 487.3 and 495.2 eV originating from Sn^{2+} were evident.[40,41] These collectively refer to the dissociations of polar $-CF_3$ and $-SO_3$ to a nonpolar surface, suggesting the development of negative tone hybrid n-CARs in the presence of an aqueous developer.

The hybrid polymer resist development, patterning, and exposure mechanism provide a platform for MAPDST-*co*-ADSM (93:07) as a potential resist for sub-15 nm technology node. Table 2 shows the summary of newly developed MAPDST-*co*-ADSM and compares it with commercially available HR e-beam resists. This aforementioned study suggests that MAPDST-*co*-ADSM HR e-beam resist is shown as a potential candidate to meet the set criterion for resist technology.

4. CONCLUSIONS

To conclude, three organic−inorganic hybrids were synthesized by the free radical copolymerization of a photosensitive sulfonium containing organic monomer MAPDST with Sn-containing monomer ADSM at different feed ratios. These copolymers acted as nonchemically amplified negative tone resists and patterned <15 nm line features with different line/space characteristics when exposed to the electron beam. The modulation in the ADSM feed ratio resulted in MAPDST-*co*-ADSM copolymers with different tin content, which eventually led to varied sensitivity toward an electron beam. Mechanistic investigations using electron beam reactivity studies revealed the formation of new carbon functionalities with C−S, C−F, etc., linkages in the exposed regions of the resist, which indicated overall transformation of the resist from hydrophilic (ionic) to hydrophobic (covalent) upon exposure. The change in polarity resulted in well-developed negative tone ~12 nm patterns under standard processing conditions. We believe the present MAPDST-*co*-ADSM resist that have the capability of patterning sub-15 nm features under electron beam exposure could be a potential candidate for EUVL applications.

ASSOCIATED CONTENT

Supporting Information

The Supporting Information is available free of charge at https://pubs.acs.org/doi/10.1021/acsapm.0c00005.

> Nuclear magnetic resonance (NMR) spectroscopy of MAPDST monomer unit (Figure S1); ADSM monomer unit (Figure S2); ^{1}H NMR and ^{19}F NMR of MAPDST-*co*-ADSM resist A (Figures S3 and S4), resist B (Figures S5 and S6), and resist C (Figures S7 and S8), XPS of MAPDST-*co*-ADSM resist A (Figure S9), resist B (Figure S10), and resist C (Figure S11); ICP OES data of MAPDST-*co*-ADSM resists A−C (Figure S12); TGA and DSC of MAPDST-*co*-ADSM resist B (Figure S13); GPC spectrum of resist A−C (Figures S14−S16); FTIR spectrum of MAPDST-*co*-ADSM resist A (Figure S17); LER/LWR analysis of HR patterning (Figure S18); calculation procedure for determining polymer microstructures ratio in resist A/B/C (Figure S19) (PDF)

AUTHOR INFORMATION

Corresponding Authors

Satinder K. Sharma − *School of Computing and Electrical Engineering (SCEE), Indian Institute of Technology (IIT) Mandi, Mandi, Himachal Pradesh 175005, India*; orcid.org/0000-0001-9313-5550; Phone: +91 1905-267134; Email: satinder@iitmandi.ac.in; Fax: 1905-267009

Kenneth E. Gonsalves − *School of Basic Sciences (SBS), Indian Institute of Technology (IIT) Mandi, Mandi, Himachal Pradesh 175005, India*; Email: kenneth@iitmandi.ac.in

Authors

Jerome Peter – *School of Computing and Electrical Engineering (SCEE), Indian Institute of Technology (IIT) Mandi, Mandi, Himachal Pradesh 175005, India*

Mohamad G. Moinuddin – *School of Computing and Electrical Engineering (SCEE), Indian Institute of Technology (IIT) Mandi, Mandi, Himachal Pradesh 175005, India*

Subrata Ghosh – *School of Basic Sciences (SBS), Indian Institute of Technology (IIT) Mandi, Mandi, Himachal Pradesh 175005, India;* orcid.org/0000-0002-8030-4519

Complete contact information is available at: https://pubs.acs.org/10.1021/acsapm.0c00005

Notes

The authors declare no competing financial interest.

■ ACKNOWLEDGMENTS

The authors thank the Department of Science and Technology (DST) and Technology Systems Development Program (TSDP), India, for the financial support under sanctioned project reference number DST/TSG/AMT/2015/634. M.G.M thanks the Ministry of Electronics & Information Technology for a Junior Research Fellowship under the Visvesvaraya Ph.D Scheme. The authors acknowledge the Centre for Design and Fabrication of Electronic Devices (C4DFED); Class 100 cleanroom facility, Indian Institute of Technology (IIT) Mandi, India, for various sample preparation facilities and state of the art EBL patterning facilities for lithography work. The authors thank Advance Material Research Center (AMRC), Indian Institute of Technology (IIT) Mandi, India, for materials characterizations.

■ REFERENCES

(1) Robinson, A.; Lawson, R. Materials and Processes for Next Generation Lithography. In *Frontiers of Nanoscience*; Palmer, R. E., Ed.; Elsevier, 2016.

(2) Li, L.; Liu, X.; Pal, S.; Wang, S.; Ober, C. K.; Giannelis, E. P. Extreme ultraviolet resist materials for sub-7 nm patterning. *Chem. Soc. Rev.* **2017**, *46*, 4855–4866.

(3) ITRS. *The International Technology Roadmap for Semiconductors*. 2015. http://www.itrs.net.

(4) Ghosh, S.; Pradeep, C. P.; Sharma, S. K.; Reddy, P. G.; Pal, S. P.; Gonsalves, K. E. Recent Advances in Non-Chemically Amplified Photoresists for Next Generation IC Technology. *RSC Adv.* **2016**, *6*, 74462–74481.

(5) Bespalov, I.; Zhang, Y.; Haitjema, J.; Tromp, R. M.; van der Molen, S. J.; Brouwer, A. M.; Jobst, J.; Castellanos, S. October 6, 2019, arXiv:1910.02511v1 .

(6) Mojarad, N.; Hojeij, M.; Wang, L.; Gobrecht, J.; Ekinci, Y. Single-Digit-Resolution Nanopatterning with Extreme Ultraviolet Light for the 2.5 nm Technology Node and Beyond. *Nanoscale* **2015**, *7*, 4031–4037.

(7) Wu, B.; Kumar, A. Extreme ultraviolet lithography: A review. *J. Vac. Sci. Technol. B* **2007**, *25*, 1743.

(8) Ito, H. Chemical amplification resists for microlithography. *Adv. Polym. Sci.* **2005**, *172*, 37–245.

(9) Moon, S. Y.; Kim, J. M. Chemistry of Photolithographic Imaging Materials Based on the Chemical Amplification Concept. *J. Photochem. Photobiol., C* **2008**, *8*, 157–173.

(10) Mojarad, N.; Gobrecht, J.; Ekinci, Y. Beyond EUV lithography: a comparative study of efficient photoresists performance. *Sci. Rep.* **2015**, *5*, 9235.

(11) Reddy, P. G.; Mamidi, N.; Kumar, P.; Sharma, S. K.; Ghosh, S.; Gonsalves, K. E.; Pradeep, C. P. Design, development, EUVL applications and nano mechanical properties of a new HfO_2 based hybrid non-chemically amplified resist. *RSC Adv.* **2016**, *6*, 67143–67149.

(12) Yu, A.; Liu, H.; Blinco, J. P.; Jack, K. S.; Leeson, M.; Younkin, T. R.; Whittaker, A. K.; Blakey, I. Patterning of Tailored Polycarbonate Based Non-Chemically Amplified Resists Using Extreme Ultraviolet Lithography. *Macromol. Rapid Commun.* **2010**, *31*, 1449–1455.

(13) Lawrie, K. J.; Blakey, I.; Blinco, J. P.; Cheng, H. H.; Gronheid, R.; Jack, K. S.; Pollentier, I.; Leeson, M. J.; Younkin, T. R.; Whittaker, A. K. Chain Scission Resists for Extreme Ultraviolet Lithography Based on High Performance Polysulfone-Containing Polymers. *J. Mater. Chem.* **2011**, *21*, 5629–5637.

(14) Fujita, J.; Ohnishi, Y.; Ochiai, Y.; Matsui, S. Ultrahigh resolution of calixarene negative resist in electron beam lithography. *Appl. Phys. Lett.* **1996**, *68*, 1297–1299.

(15) Cardineau, B.; Del Re, R.; Marnell, M.; Al-Mashat, H.; Vockenhuber, M.; Ekinci, Y.; Sarma, C.; Freedman, D. A.; Brainard, R. L. Photolithographic Properties of Tin-Oxo Clusters Using Extreme Ultraviolet Light (13.5 nm). *Microelectron. Eng.* **2014**, *127*, 44–50.

(16) Shi, X.; Prewett, P.; Huq, E.; Bagnall, D. M.; Robinson, A. P. G.; Boden, S. A. Helium ion beam lithography on fullerene molecular resists for sub-10 nm patterning. *Microelectron. Eng.* **2016**, *155*, 74–78.

(17) Telecky, A.; Xie, P.; Stowers, J.; Grenville, A.; Smith, B.; Keszler, D. A. Photopatternable inorganic hardmask. *J. Vac. Sci. Technol., B: Nanotechnol. Microelectron.: Mater., Process., Meas., Phenom.* **2010**, *28*, C6S19–22.

(18) Reddy, P. G.; Thakur, N.; Lee, C.-L.; Chien, S.-W.; Pradeep, C. P.; Ghosh, S.; Tsai, K.-Y.; Gonsalves, K. E. Heavy metal incorporated helium ion active hybrid non-chemically amplified resists: Nano-patterning with low line edge roughness. *AIP Adv.* **2017**, *7*, 085314.

(19) Sharma, S. K.; Moinuddin, M. G.; Reddy, P. G.; Pradeep, C. P.; Ghosh, S.; Gonsalves, K. E. Evaluation of high-resolution and sensitivity of n-CAR hybrid resist for sub-16nm or below technology node. *Proc. SPIE* **2018**, 105831Q.

(20) Singh, V.; Satyanarayana, V. S. V.; Sharma, S. K.; Ghosh, S.; Gonsalves, K. E. Towards novel non-chemically amplified (n-CARS) negative resists for electron beam lithography applications. *J. Mater. Chem. C* **2014**, *2*, 2118–2122.

(21) Enomoto, S.; Yoshino, T.; Machida, K.; Kozawa, T. Effects of an organotin compound on radiation-induced reactions of extreme-ultraviolet resists utilizing polarity change and radical crosslinking. *J. J. Appl. Phys.* **2019**, *58*, 016504.

(22) Miyoshi, H.; Taniguchi, J. Fabricating a high-resolution mask with improved line-edge roughness by using a nonchemically amplified resist and a postexposure bake. *J. Vac. Sci. Technol., B: Nanotechnol. Microelectron.: Mater., Process., Meas., Phenom.* **2015**, *33*, 06FD05.

(23) Kwang-Woo, C.; Prabhu, V. M.; Lavery, K. A.; Lin, E. K.; Wu, W.; Woodward, J. T.; Leeson, M. J.; Cao, H. B.; Chandhok, M.; Thompson, G. Effect of photo-acid generator concentration and developer strength on the patterning capabilities of a model EUV photoresist. *Advances in Resist Materials and Processing Technology XXIV*; International Society for Optics and Photonics: Bellingham, WA, 2007; Vol. *6519*, p 651943.

(24) Summit Litho Image Analysis Software. *SuMMIT Software Division of EUV Technology*. 2009. http://www.euvl.com/summit/.

(25) Krysak, M.; Trikeriotis, M.; Schwartz, E.; Lafferty, N.; Xie, P.; Smith, B.; Zimmerman, P.; Montgomery, W.; Giannelis, E.; Ober, C. K. Development of an inorganic nanoparticle photoresist for EUV, e-beam, and 193nm lithography. *Proc. SPIE* **2011**, *7972*, 79721C.

(26) Del Re, R.; Passarelli, J.; Sortland, M.; Cardineau, B.; Ekinci, Y.; Buitrago, E.; Neisser, M.; Freedman, D. A.; Brainard, R. L. Low-line edge roughness extreme ultraviolet photoresists of organotin carboxylates. *J. Micro/Nanolithogr., MEMS, MOEMS* **2015**, *14* (4), 043506.

(27) Passarelli, J.; Murphy, M.; Del Re, R.; Sortland, M.; Dousharm, L.; Vockenhuber, M.; Ekinci, Y.; Neisser, M.; Freedman, D. A.;

Brainard, R. L. High-Sensitivity Molecular Organometallic Resist for EUV (MORE). *Proc. SPIE* **2015**, *9425*, 94250T.

(28) Blunden, S. J.; Chapman, A. H. The environmental degradation of organotin compounds-a review. *Environ. Technol. Lett.* **1982**, *3*, 267−272.

(29) Reddy, P. G.; Pal, S. P.; Kumar, P.; Pradeep, C. P.; Ghosh, S.; Sharma, S. K.; Gonsalves, K. E. Polyarylenesulfonium Salt as a Novel and Versatile Nonchemically Amplified Negative Tone Photoresist for High-Resolution Extreme Ultraviolet Lithography Applications. *ACS Appl. Mater. Interfaces* **2017**, *9*, 17−21.

(30) Gangnaik, S.; Georgiev, Y. M.; Holmes, J. D. New Generation Electron Beam Resists: A Review. *Chem. Mater.* **2017**, *29*, 1898−1917.

(31) Reddy, P. G.; Moinuddin, M. G.; Joseph, A. M.; Nandi, S.; Ghosh, S.; Pradeep, C. P.; Sharma, S. K.; Gonsalves, K. E. Ferrocene Bearing Non-ionic Poly-aryl Tosylates: Synthesis, Characterization and Electron Beam Lithography Applications. *J. Photopolym. Sci. Technol.* **2018**, *31*, 669−678.

(32) Satyanarayana, V. S. V.; Kessler, F.; Singh, V.; Scheffer, F. R.; Weibel, D. E.; Ghosh, S.; Gonsalves, K. E. Radiation-Sensitive Novel Polymeric Resist Materials: Iterative Synthesis and Their EUV Fragmentation Studies. *ACS Appl. Mater. Interfaces* **2014**, *6*, 4223−4232.

(33) Singh, V.; Satyanarayana, V. S. V.; Batina, N.; Reyes, I. M.; Sharma, S. K.; Kessler, F.; Scheffer, F. R.; Weibel, D. E.; Ghosh, S.; Gonsalves, K. E. Performance evaluation of nonchemically amplified negative tone photoresists for e-beam and EUV lithography. *J. Micro/Nanolithogr., MEMS, MOEMS* **2014**, *13* (4), 043002.

(34) Shi, X.; Prewett, P.; Huq, E.; Bagnall, D. M.; Robinson, A. P. G.; Boden, S. A. Helium ion beam lithography on fullerene molecular resists for sub-10 nm patterning. *Microelectron. Eng.* **2016**, *155*, 74−78.

(35) Kim, J.; Chao, W.; Griedel, B.; Liang, X.; Lewis, M.; Hilken, D.; Olynick, D. Understanding the base development mechanism of hydrogen silsesquioxane. *J. Vac. Sci. Technol. B* **2009**, *27* (6), 2628−2634.

(36) Wi, J. S.; Lee, H. S.; Kim, K. B. Enhanced Development Properties of IPA (Isopropyl Alcohol) on the PMMA Electron Beam Resist. *Electronic Mater. Lett.* **2007**, *3*, 1−5.

(37) Yasin, S.; Hasko, D. G.; Ahmed, H. Comparison of MIBK/IPA and water/IPA as PMMA developers for electron beam nanolithography. *Microelectron. Eng.* **2002**, *61*, 745−753.

(38) Kumar, P.; Reddy, P. G.; Sharma, S. K.; Ghosh, S.; Pradeep, C. P.; Gonsalves, K. E. Enhanced mechanical properties of the high-resolution EUVL patterns ofhybrid photoresists containing hexafluoroantimonate. *Microelectron. Eng.* **2018**, *194*, 100−108.

(39) Guruprasad Reddy, P.; Kumar, P.; Ghosh, S.; Pradeep, C. P.; Sharma, S. K.; Gonsalves, K. E. Organic-inorganic hybrid photoresists containing hexafluoroantimonate: design, synthesis and high resolution EUV lithography studies. *Mater. Chem. Front.* **2017**, *1*, 2613−2619.

(40) Stowers, J.; Keszler, D. A. High resolution, high sensitivity inorganic resists. *Microelectron. Eng.* **2009**, *86*, 730−733.

(41) Gonsalves, K. E.; Ghosh, S.; Pradeep, C. P.; Reddy, P. G.; Sharma, S. K.; Pal, S. P. Resist Technology Based on Polyarylene Sulphide: (PAS) as a Unique Polymer Material for Semi Conductor Fabrication Technology. *RSC Adv.* **2016**, *6*, 74462.

(42) Yang, J. K.; Cord, B.; Duan, H.; Berggren, K. K.; Klingfus, J.; Nam, S. W.; Kim, K. B.; Rooks, M. J. Understanding of hydrogen silsesquioxane electron resist for sub-5-nm-half-pitch lithography. *J. Vac. Sci. Techol. B* **2009**, *27*, 2622−2627.

(43) Thoms, S.; Macintyre, D. S. Investigation of CSAR 62, a new resist for electron beam lithography. *J. Vac. Sci. Technol., B: Nanotechnol. Microelectron.: Mater., Process., Meas., Phenom.* **2014**, *32*, 06FJ01.

(44) Nagai, T.; Nakagawa, H.; Naruoka, T.; Dei, S.; Tagawa, S.; Oshima, A.; Nagahara, S.; Shiraishi, G.; Yoshihara, K.; Terashita, Y.; Minekawa, Y.; Buitrago, E.; Ekinci, Y.; Yildirim, O.; Meeuwissen, M.; Hoefnagels, R.; Rispens, G.; Verspaget, C.; Maas, R. Novel High Sensitivity EUV Photoresist for Sub-7 nm Node; *J. Photopolym. Sci. Technol.* **2016**, *29*, 475−478.

(45) Hu, W.; Sarveswaran, K.; Lieberman, M.; Bernstein, G. H. Sub-10 nm electron beam lithography using cold development of poly(methylmethacrylate). *J. Vac. Sci. Technol., B: Microelectron. Process. Phenom.* **2004**, *22*, 1711−1716.

(46) Bilenberg, B.; Jacobsen, S.; Schmidt, M. S.; Skjolding, L. H. D.; Shi, P.; Bøggild, P.; Tegenfeldt, J. O.; Kristensen, A. High Resolution 100 KV Electron Beam Lithography in SU-8. *Microelectron. Eng.* **2006**, *83*, 1609−1612.

(47) Matejka, M. Behavior of SU-8 epoxy based negative uv-photoresist as negative tone resist for electron-beam lithography.

(48) Canalejas-Tejero, V.; Carrasco, S.; Navarro-Villoslada, F.; Garcia Fierro, J. L.; Capel-Sanchez, M. d. C.; Moreno-Bondi, M. C.; Barrios, C. A. Ultrasensitive non-chemically amplified low-contrast negative electron beam lithography resist with dual-tone behaviour. *J. Mater. Chem. C* **2013**, *1*, 1392−1398.

(49) Gangnaik, A.; Georgiev, Y. M.; Holmes, J. D. Correlation of lithographic performance of the electron beam resists SML and ZEP with their chemical structure. *J. Vac. Sci. Technol., B: Nanotechnol. Microelectron.: Mater., Process., Meas., Phenom.* **2015**, *33*, 041601.